

## A new rabbit model for the study on cervical compressive myelopathy

Tsukasa Kanchiku<sup>a,\*</sup>, Toshihiko Taguchi<sup>a</sup>, Kazuo Kaneko<sup>a</sup>, Hiroshi Yonemura<sup>a</sup>,  
Shinya Kawai<sup>a</sup>, Toshikazu Gondo<sup>b</sup>

<sup>a</sup> Department of Orthopedic Surgery, Yamaguchi University School of Medicine, 1-1-1 Minami-Kogushi, Ube, Yamaguchi 755-8505, Japan

<sup>b</sup> First Department of Pathology, Yamaguchi University School of Medicine, 1-1-1 Minami-Kogushi, Ube, Yamaguchi 755-8505, Japan

Received 28 December 1999; accepted 19 January 2000

### Abstract

Development process and pathology of myelopathy due to chronic spinal cord compression have not been fully elucidated. This study was conducted in order to establish an experimental model which can efficiently produce myelopathy and be useful in the studies on myelopathy due to chronic spinal cord compression. Under electrophysiological monitoring of the spinal cord, anterior compression was produced on C5 using a plastic screw. Two weeks later, a plastic plate was inserted under the C5 arch. For the subsequent 10 months on average, walking pattern and MR images were periodically monitored. Before the sacrifice, electrophysiological test was performed and then histopathological examination was done. Palsy appeared at 5 months on average after the addition of posterior compression. Mean compression ratio of the spinal cord calculated on MR images was 34%. All animals with compression showed a high intramedullary signal intensity, and the mean contrast-to-noise ratio (CNR) in the compressed area was 49%. Electrophysiological test showed a significant decrease in the amplitude of spinal cord evoked potentials (SCEPs) at the given compression level. Histology showed flattening of the anterior horn, disappearance and necrosis of anterior horn cells in the gray matter; and demyelination and axonal degeneration in the white matter. The antero-posterior compression produces the condition of spinal canal stenosis. Repeated antero-posterior compression to the spinal cord is important in establishing myelopathy. The present animal model was evaluated to be useful in the studies on myelopathy. © 2001 Orthopaedic Research Society. Published by Elsevier Science Ltd. All rights reserved.

### Introduction

Various animal experiments on spinal cord injury have been conducted in order to deepen the understanding on the pathology of compressed lesions. However, these experiments usually utilized the models of acute symptoms produced by weight bearing and/or clamps, and there have been a few studies on chronic compression. Major symptom of cervical spondylotic myelopathy is spinal paralysis which is generated by the osteoarthropathic changes of the spine, and the spine presents such morphological characteristics as cervical disk degeneration, osteophyte formation [1,4,25,37,39,41], hypertrophic yellow ligament [26,29,36], cervical spinal stenosis [8–10,27,29,42], and abnormal mobility of the cervical spine [30]. In regard to the generation process of cord symptoms, there have been two major assumptions. One emphasizes tissue damages caused by mechanical compression given to the spinal cord [4,39,41], and the other

one emphasizes circulatory disorders within the spinal cord. Some researchers proposed a combination of these two hypothesis [15,18]. However pathology of myelopathy has remained unclear because of the absence of an appropriate animal model for the studies.

In the present study, we tried to establish a rabbit model with typical clinical characteristics of cervical compressive myelopathy, in which disk and facet were maintained in order to preserve mobility of the cervical spine, and compression was given to a single intervertebral space using a plastic screw from the front side and a plate from the dorsal side. In this model, spinal cord compression is produced when the cervical spine moves. With MRI, electrophysiological test, and histological examination, we confirmed that this model efficiently produces delayed myelopathy.

### Materials and methods

#### *Chronic compression model*

Thirteen 12-week old Japanese white rabbits (body weights: 2.6–3.0 kg, mean: 2.8 kg, male) were used in this study. The animals

\* Corresponding author. Tel.: +81-836-22-2268; fax: +81-836-22-2267.

E-mail address: y-ortho@po.cc.yamaguchi-u.ac.jp (T. Kanchiku).

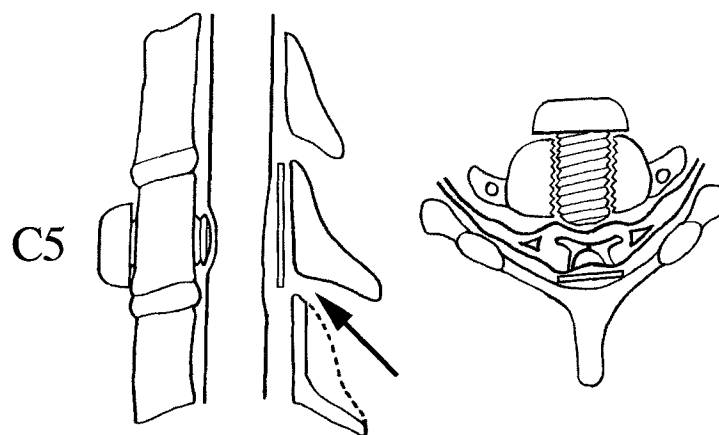


Fig. 1. Illustration of the rabbit model. A plastic screw is inserted into the anterior body of the C5 vertebra, and a plastic plate placed posteriorly beneath the C5 lamina is inserted from the interlamina space (←). The spinous process of the C6 lamina is resected to insert the plastic plate into the cervical canal parallel to the C5 lamina.

were given an ordinary laboratory diet and water. They were housed in cages at 16–20°C with a 12-h-light/12-h-dark cycle. This experiment was reviewed by the Committee of the Ethics on Animal Experiment in Yamaguchi University School of Medicine and carried out under the control of the Guideline for Animal Experiment in Yamaguchi University School of Medicine and The Law (No. 105) and Notification (No. 6) of the Government. Eight animals underwent sub-clinical cervical cord compression produced by plastic devices. The route of drip infusion was set on the auricular vein, and the surgery was performed under the i.v. anesthesia using 50 mg/kg of pentobarbiturate (Nembutal, Dainippon Pharmaceuticals, Japan). Tubation was not performed, and oxygen was given using a mask. The rabbit was positioned on the special operating table lying on the back, immobilized, hair on the cervical area was shaved, and an transverse incision reaching to the anterior part of the fifth cervical vertebra was aseptically made by avoiding the trachea and esophagus. An X-ray film of the cervical spine was taken intraoperatively to ascertain the pressure level. A hole was produced slightly below the center of the C5 vertebral body by using an electric drill with a diamond bur (3 mm in diameter), its depth was measured with a micrometer, the area around the hole was tapped, a plastic screw (4 mm in diameter, 0.7 mm of pitch) was placed into the hole at a rate of 0.7 mm/min to produce approximately 1 mm compression measured from the posterior side of the vertebral body. This was determined as anterior compression. During the surgery, electrophysiological monitoring of the spinal cord was conducted, and no changes in wave patterns were confirmed. After the surgery, oxygen was administered until the overall condition was stabilized, and antibiotics (Cefazolin Sodium, Fujisawa Pharmaceuticals, Japan) were i.v. administered. In the following day, walking pattern was monitored, and no paralysis was confirmed. Approximately 2 weeks after producing the anterior compression, the rabbits were anesthetized in the same manner, a longitudinal incision was made on the back centered on the spinous process of the fifth cervical spine and the paravertebral muscles were stripped from the spinous process. The spinous process of the sixth cervical spine was resected, the vertebral arch was slightly shaved with an airtome, the yellow ligament between the vertebral arch of C5 and C6 was resected, and then a plastic plate (7 mm height × 4 mm width × 0.5 mm thickness) was inserted horizontally below the arch of C5 to produce posterior compression (Fig. 1). Before and during this surgery, electrophysiological monitoring was performed, and no changes in wave patterns were confirmed. After the surgery, oxygen and antibiotics were administered in the same manner as in the previous surgery. In the following day, walking pattern was confirmed to be normal. If any abnormality was found in the electrophysiological monitorings or in the walking pattern on the following day, the rabbit was considered to have acute compression, and excluded from this study.

#### Control animal model

Surgery was performed in the above-mentioned manner. The screw was removed immediately after producing anterior compression. The plate was inserted 2 weeks later, and it was also removed immediately. Five control animals were prepared, and all animals were sacrificed at 8 months after surgery for gross observation and histology.

#### Paralysis (motor function) evaluation

Severity of paralysis due to spinal cord compression was evaluated in terms of motor function by using the modification of Tarlov's classification [38] (Table 1). Evaluation was made before and immediately after the surgery, and once a week thereafter.

#### Electrophysiological evaluation

Three types of spinal cord evoked potentials (SCEPs) were recorded before and during the surgery, and before the sacrifice, for all animals. SCEPs after electric stimulation to the peripheral nerve (Pn-SCEPs), SCEPs after electric stimulation to the spinal cord (Sp-SCEPs) and SCEPs after electric stimulation to the brain (Br-SCEPs) were measured using Nicolet Viking IV (Nicolet Biomedical, USA) (Fig. 2). Stimulation was given at 3.7 Hz of frequency, 0.2 ms of duration, 1.5–3 times higher strength than the maximum stimuli, and addition was made 100 times on average. SCEPs were recorded with needle electrodes (13R25, Dantec, Denmark) inserted into the ligamentum flavum at each level of the interlamina space. The reference electrodes were inserted subcutaneously in the posterior neck. For recording Pn-SCEPs, two needle electrodes for stimulation of the median nerve were inserted at the wrist joint percutaneously. For recording Sp-SCEPs, two needle electrodes for stimulation of the thoracic spinal cord were inserted into the ligamentum flavum at thoracic spine subcutaneously. For recording Br-SCEPs, two needle electrodes

Table 1  
Modified Tarlov's classification for motor functions

Grade	
0	Unable to have voluntary movements
1	Perceptible movement at joints, the hindlimbs follow
2	Good movement at joints but unable to stand up
3	Can stand up and walk, but unable to start running quickly
4	Normal

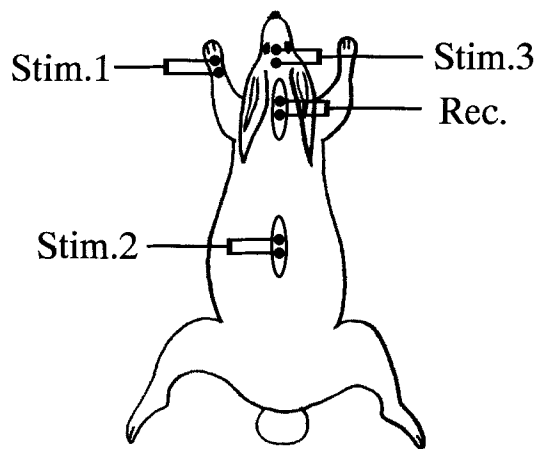


Fig. 2. The protocol of SCEPs measurement. Pn-SCEPs are spinal cord evoked potentials after electric stimulation to the median nerve (Stim. 1). Sp-SCEPs are spinal cord evoked potentials after electric stimulation to the thoracic spinal cord (Stim. 2). Br-SCEPs are spinal cord evoked potentials after electric stimulation to motor area of the brain (Stim. 3).

for stimulation of the brain were inserted into cerebral epidural space at motor area from a hole of the cephalic bone produced by using an electric drill with a diamond bur (3 mm in diameter). The amplitude ratio was obtained in the following way from the wave patterns at sacrifice. For Pn-SCEPs, the ratio was determined as the 'amplitude of the wave obtained from the compressed intervertebral space' divided by the 'amplitude of the wave obtained from intact C6/7'. For Sp-SCEPs, the ratio was determined as the 'amplitude of the wave obtained from the compressed intervertebral space' divided by the 'amplitude of the wave obtained from the space at one level lower', and for Br-SCEPs, as the 'amplitude of the wave obtained from the compressed intervertebral space' divided by the 'amplitude of the wave obtained from the space at one level upper'.

#### MRI

MR images were obtained using 1.5 T superconductive coil, Magnetom Vision (Siemens, Germany) for clinical use, within one month after surgery, then once in 2–3 months until when paralysis occurred, and before the sacrifice. The animal was i.v. anesthetized using pentobarbiturate, positioned on the coil for human knee joint lying prone, and immobilized. T1-weighted (TR 350 ms, TE 15 ms) and T2-weighted (TR 2000 ms, TE 100–120 ms) sagittal and axial images were obtained using the Spin Echo method. All imagings were performed at acquisition 2–9. Sagittal sections were obtained with 2 mm of slice thickness, 256 × 256 of matrix, and 200 × 100 mm of FOV. Axial images were obtained with 3 mm of slice thickness, 512 × 208 of matrix, and 135 × 135 mm of FOV. Compression ratio and cross-sectional area were measured on the T1-weighted axial sections passing through the area which received the maximum compression level (maximum compression area). Presence or absence of intramedullary high signal intensity area was examined using T2-weighted images. In order to quantify the intramedullary intensity, contrast-to-noise ratio (CNR) (%) was obtained as the 'intramedullary signal intensity at the maximum compression area in T2-weighted sagittal images' divided by the 'intramedullary signal intensity in non-compression area'.

#### Histology

Spinal cord was extirpated immediately after sacrifice, microwave-fixed, immersed into a fixing solution, deionized using cacodylate buffer, immersed in phosphate buffer sulfate solution, and each segment was prepared into 5 mm-thick slices. The slices were paraffin embedded, underwent HE staining, Kluver–Barrera staining, PTAH staining, Elastic van Gieson (EVG) staining, and immunochemical staining, and used for the histologic examination.

#### Statistical analysis

Statistical analysis was conducted using Student's *t*-test, and *P* values less than 0.01 were considered statistically significant.

#### Results

Mean post-operative monitoring period was 10 months (range, 6–12 months), and paralysis appeared at 5 months (range, 3–6 months) after surgery. The final motor function level was Grade 3 in 7 animals and Grade 4 in one. In the control animals, the motor function was normal and did not change. Electrophysiological monitoring before sacrifice showed significant decreases in the amplitudes of Sp-SCEPs, Pn-SCEPs, and Br-SCEPs on the compressed area in comparison to the controls (Fig. 3 and Table 2). Mean cross-sectional area of the spinal cord obtained from T1-weighted axial images was 22 mm<sup>2</sup>; and mean compression ratio was 34% which was significantly different from the controls (Table 3). In T2-weighted sagittal images, hyperintensity area was found in the medullary of the compressed area, while in T2-weighted axial images, intensities of the white and gray matters on the compressed area were higher than those in the areas without compression (Fig. 4). There was a significant group difference on the CNR (Table 4). Histologically, the gray matter was associated with the flattening of the anterior horn, and disappearance and necrosis of the anterior horn cells, while the white matter showed spongy degeneration, axonal degeneration, and mild demyelination (Figs. 5 and 6). In addition, mild gliosis was found mainly on the gray matter. In the controls, there were no histological abnormalities.

#### Discussion

##### *Previous spinal cord compression experiments, and the evaluation of our animal model*

To date, chronic compression to the spinal cord has been examined by gradually increasing compression levels using balloon [38] or metal screws [32,35], or in the epidural tumor models [3,11,12,23,24,40]. Speed and degree of compression given by a balloon or metal screws are easily controllable, but additional compression could cause spinal cord injury, which then tends to result in acute spinal cord compression. Tumors [3,11,12,23,24,40] and expandable plastic [6,7,14] are also utilized. Most tumor models utilized metastatic tumors, therefore the mode of compression would vary according to the shape of the tumor nodule. In addition, tumor itself would cause tissue damages. These models are suited to the examinations for subacute spinal cord injuries caused by severe compression.

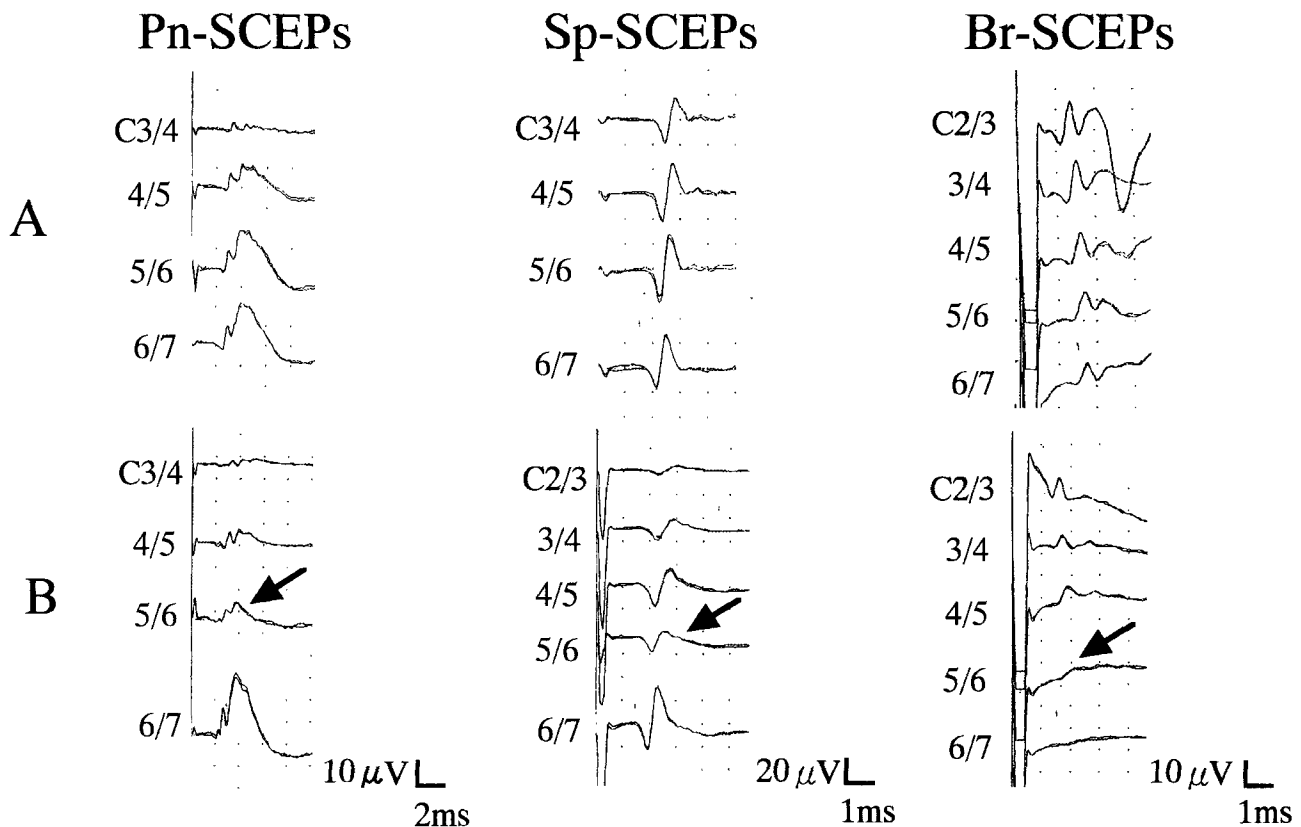


Fig. 3. SCEPs obtained before sacrifice: (A) control group; (B) Case No. 3 which had C5 compression. Pn-SCEPs, Sp-SCEPs and Br-SCEPs showed abnormality at C5 level in the Case No. 3. Amplitude ratio was 15% for Pn-SCEPs, 17% for Sp-SCEPs, and 30% for Br-SCEPs.

Table 2  
Amplitude ratio of SCEPs<sup>a</sup>

	Animals with compression	Control animals
Sp-SCEPs*	50 ± 24	100 ± 0
Pn-SCEPs**	42 ± 17	105 ± 6
Br-SCEPs***	32 ± 10	90 ± 8

<sup>a</sup> Figures represent mean ratio ± S.D. Sp-SCEPs: The ratio was determined as the 'amplitude of the wave obtained from the compressed intervertebral space' divided by the 'amplitude of the wave obtained from the space at one level lower'. Pn-SCEPs: The ratio was determined as the 'amplitude of the wave obtained from the compressed intervertebral space' divided by the 'amplitude of the wave obtained from intact C6/7'. Br-SCEPs: The ratio was determined as the 'amplitude of the wave obtained from the compressed intervertebral space' divided by the 'amplitude of the wave obtained from the space at one level upper'.

\*  $P < 0.001$ .

\*\*  $P < 0.01$ .

\*\*\*  $P < 0.0001$ .

In our model, surgical treatment is not performed on intervertebral disks and facets, and compression is given to a single intervertebral space. This maintains a relatively wide range of vertebral motions. In our model, the spinal cord is thought to be compressed from the front and dorsal sides during the movement of cervical spine, and this produces conditions similar

Table 3  
MRI findings on cross-sectional area and compression ratio<sup>a</sup>

	Animals with compression	Control animals
Cross-sectional area (mm <sup>2</sup> )	22 ± 3	23 ± 1
Compression ratio (%) <sup>*</sup>	34 ± 5	52 ± 5

<sup>a</sup> Compression ratio was obtained as the ratio of the antero-posterior diameter to the transverse diameter [38]. Figures represents mean ± S.D.

\*  $P < 0.01$ .

to clinical cervical spondylotic myelopathy. In 1993, Al-Mefty et al., reported a similar model of chronic compression to the spinal cord using dogs [2]. However, we used rabbits which are much easier to raise, conducted electrophysiologic monitoring during the surgery in order to confirm that the surgery did not cause paralysis on the gray and white matters, and also electrophysiologically proved that our treatment induces delayed paralysis. Severe paralysis, i.e., Grade 2 or higher, was not observed in all animals. In our present model, paralysis is produced by relatively mild chronic spinal cord compression. More severe paralysis could be produced by adjusting the degree of the anterior compression, and this point would be examined in another study.

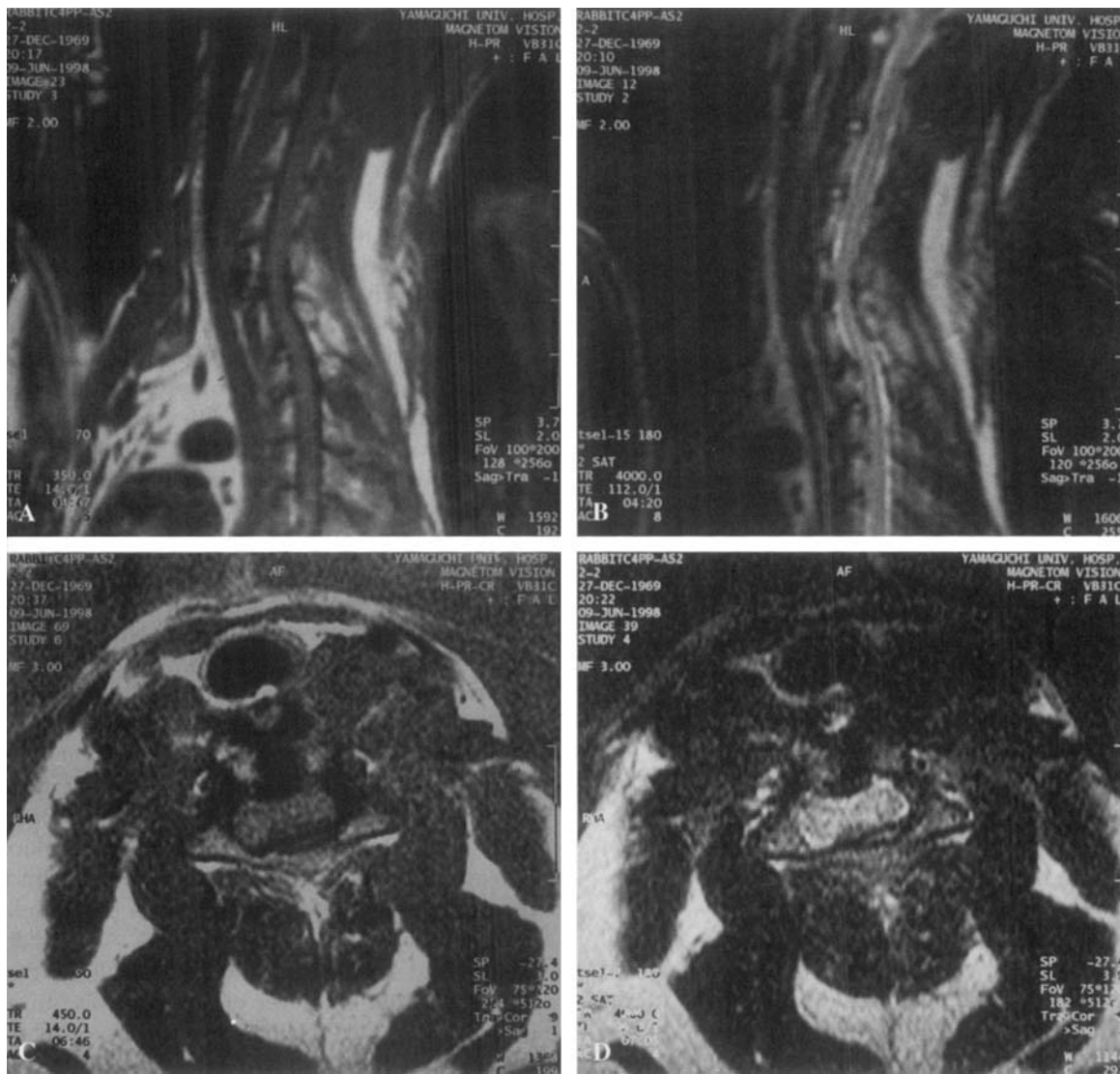


Fig. 4. MRI findings of Case No. 3. (A, B). T1- and T2-weighted sagittal image. The antero-posterior compression given to C5 level was confirmed, high intramedullary intensity was identified at the compressed area, and CNR was 47%. (C, D). T1- and T2-weighted axial image at C5 level. The C5 spinal cord was flattened due to the antero-posterior compression.

*Spinal cord compression and appearance of paralysis*

Shinomia et al. [35] gradually increased anterior compression using a metal screw, and observed that the single compression group did not show any disturbance of limb function during 50% compression of the spinal canal. Schramm et al. [32] gradually increased posterior compression level, and observed motor paralysis of the lower extremities at 66% (mean) of stenosis. These previous findings show that paralysis is difficult to induce by either anterior or posterior compression alone using a single metal screw. On the other hand, many clinical reports demonstrated narrowed diameter of the spinal canal in patients with cervical spondylotic myelopathy

[8–10,27,29,42]. Hinck et al. [17] showed that patients with spinal stenosis would easily develop myelopathy by small osteophyte and mild injury. Therefore, pre-

Table 4  
Contrast-to-noise ratio<sup>a</sup>

	Animals with compression	Control animals
T2-weighted, sagittal (%) <sup>*</sup>	49 ± 12	86 ± 4

<sup>a</sup> CNR ratio was obtained as the 'intramedullary signal intensity at the maximum compression area in T2-weighted sagittal images' divided by the 'intramedullary signal intensity in non-compression area'. Figures represents mean ± S.D.

<sup>\*</sup> P < 0.01.

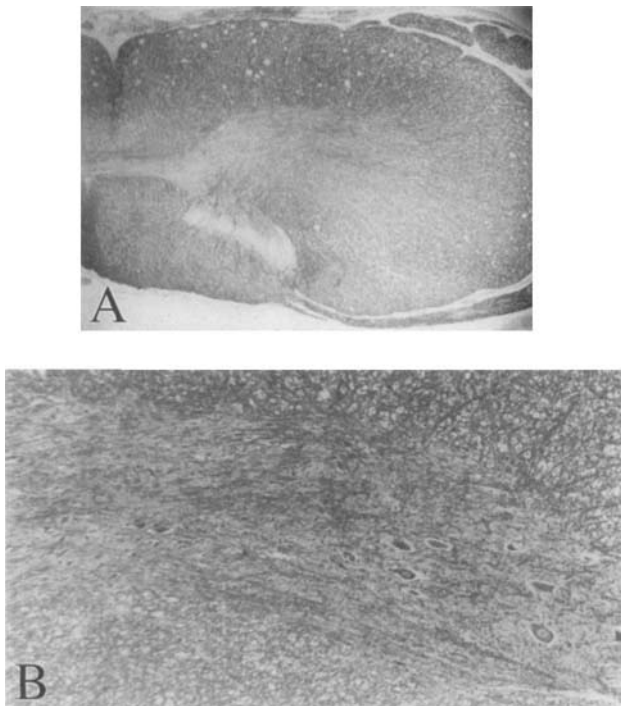


Fig. 5. Histologic findings of Case No. 3. (A) Axial section of the compressed area showed flattening of the anterior horn in the gray matter. Severe demyelination were not found in the white matter. (Kluver–Barrera staining, X4). (B) Shrinkage and degeneration of nerve cells were detected in the anterior horn (Kluver–Barrera staining, X10).

requisites of paralysis would be: (i) the spinal canal has stenosis, (ii) the epidural space and subarachnoid space are perfectly occluded, and (iii) mobility of the spine is maintained.

In our model, compression is given to one intervertebral space, and the disk and facet are maintained; the plate for posterior compression is inserted below the C5 arch and only a part of it is below the C6 arch, and range of motions is maintained. The antero-posterior compression produces the condition of spinal canal stenosis. Therefore, in our model, antero-posterior spinal cord compression is thought to be efficiently produced when the cervical spine moves, and this would be the mechanism of paralysis in this model. In the observation at sacrifice of the animals which showed only mild electrophysiologic changes of the white matter ( $n = 1$ ), the position of the plate was shifted to either the left or the right side. This is similar to the findings on 'teardrop type' patients who have spinal cord compression mainly on one side, have relatively mild symptoms, and usually have good outcomes [43]. This would be because, when anterior- or posterior-flexion of the cervical spine produces dynamic compression to the spinal cord, there is a space for the spinal cord to escape the compression, and as a result compression is not efficiently produced. Therefore, in the model preparation,

the plate for posterior compression should be carefully placed almost on the midline.

#### *Electrophysiological findings*

Spinal cord evoked potentials can be recorded safely from the cervical epidural space using a catheter electrode [33] in conscious condition or directly from posterior interlaminar space using needle electrodes intraoperatively in cervical myelopathy. Such SCEP recordings allow us to accurately determine not only the pathological condition of the spinal cord but also the symptomatic level of compression in compressive cervical myelopathy [21,31,34]. Major parameters are amplitude, wave pattern, and conductive velocity. Clinical diagnosis utilizes such index as the decrease/increase of amplitude, and types and positive changes of certain potentials. (Schramm et al. [32] produced a gradual posterior-compression model in adult cats by using a plate and forceps, and reported that SCEPs derived from the area 8–10 mm closer to the center from the compressed point showed 'killed end-potential' with 36% of compression, and its appearance was faster than that of dyskinesia.) The early components of evoked potential following median nerve stimulation recorded from the cervical cord surface in humans are composed of an initial P9 potential, a presynaptic N11 potential, and a postsynaptic N13 potential generated by large diameter afferent fibers in the deep laminae of the dorsal horn [20]. Similar wave patterns were recorded in rabbits. Amplitude at the compressed area of the model animals decreased significantly from the level of the controls. In addition, in proportion to the compression level, abnormality appeared in the order from Pn-SCEPs, Br-SCEPs, to Sp-SCEPs. Appearance of abnormality found in our model was similar to that in clinical compressive myelopathy.

#### *MRI findings*

There have been a relatively large number of MRI studies on experimental acute spinal cord injury, because there are established models. On the other hand, there have been a few MRI studies on subacute and chronic spinal cord injuries, because of the difficulty in establishing a model. Al-Mefty et al. [2] prepared chronic spinal cord compression model in dogs, obtained T2-weighted MR images, and reported intramedullary high intensity areas in a snake-eye pattern at compression site, which were indicative of cystic necrosis of the gray matter found at the time of histological study. Fukuoka et al. [14] prepared a subacute spinal cord compression model using expandable plastic, and reported that intramedullary signal intensity in T2-weighted images became stronger with the

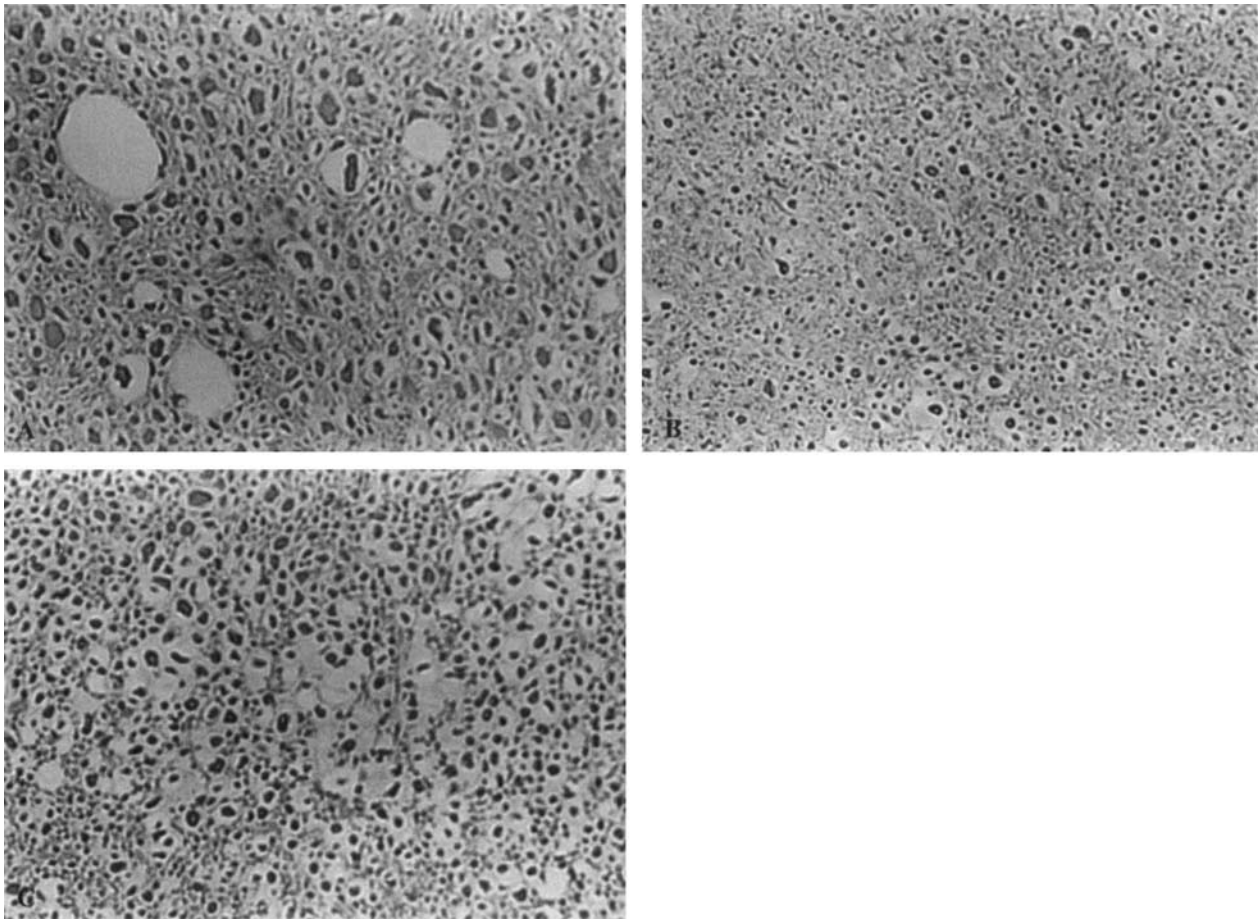


Fig. 6. Immunohistochemical findings of Case No. 5 (Neuro-filament staining, X10). (A) Anterior funiculus. (B) Lateral funiculus. (C) Posterior funiculus. In (A)–(C), axons of the anterior funiculus were well maintained, while degenerated axons were found in the lateral and posterior funiculi.

increase at the compressed area, and cases whose intramedullary signal intensity was low in T1-weighted images had higher level of compression and severe paralysis. In the present study, we found intramedullary high intensity areas at the compressed area in T2-weighted images, and the intensity quantified as the CNR was significantly high at the compressed area, and the high-intensity areas were histologically correlated to necrotic changes and gliosis in the gray matter, with demyelination and axonal degeneration in the white matter.

#### *Histological findings*

Many autopsy cases of cervical spondylotic myelopathy have been reported [5,13,19,22,27–29]. A histologic characteristic of nerves in patients with cervical spondylotic myelopathy is the distribution of degenerated lesions, i.e., demyelination and spongy degeneration are found at high compression areas, and the ascending and descending axonal degenerations derived from the degenerative changes were apparent on the lateral funiculus. In patients, degeneration of the pos-

terior funiculus could be remarkable or relatively mild, and the anterior funiculus was well maintained in all cases and all areas including high compression area. In regard to the gray matter, atrophy of the anterior horn and loss of nerve cells have been thought to occur at the early compression stage, but some researchers reported that the gray matter was maintained at the early compression stage, and the degeneration and loss of anterior horn cells, and the collapse and cavitation of the anterior horn tissue were found only in the area under severe compression. In the present study, histologic findings in our animals were similar to those found in clinical cases. The white matter had axonal degeneration, spongy degeneration and mild demyelination of the lateral funiculus, and the posterior funiculus, whereas the anterior funiculus was relatively well maintained (Fig. 6). In the gray matter, no animals had remarkable necrosis or cavity, but there was flattening of the anterior horn as well as degeneration and loss of the anterior horn cells (Fig. 5). With EVG staining, occlusion of the arteries was not detected, but some animals had veins with wall-thickening and expanded lumen in the subarachnoid space and the gray matter

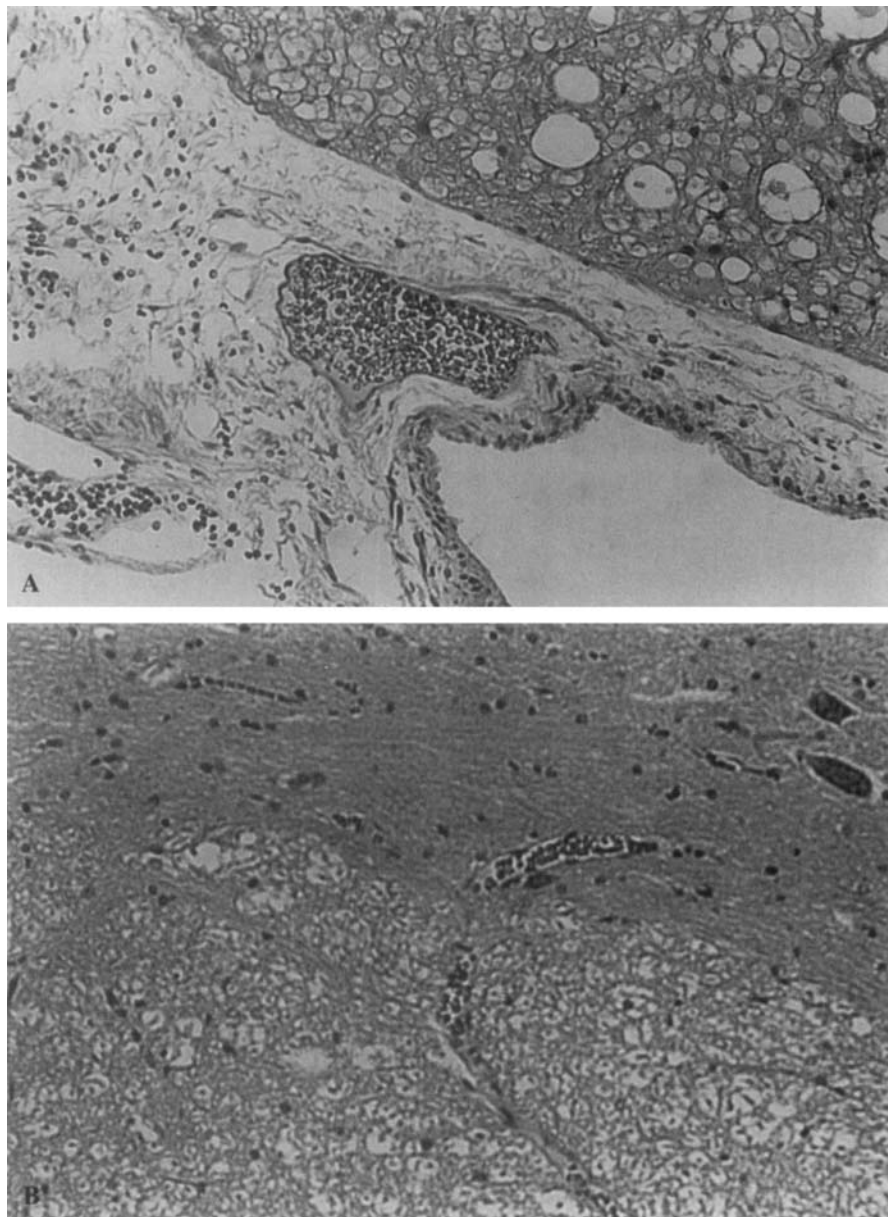


Fig. 7. (A) Wall-thickening and expanded diameter were detected in the veins of epidural space on the dorsal side (EVG staining, X10). (B) Within the medullar, there were veins with thickened wall and expanded diameter (EVG staining, X10).

(Fig. 7). Hashizume et al. [16] suggested two cyst-formation processes in the spinal cord of cervical spondylotic myelopathy patients: (i) necrosis due to venous circulatory disorders associated with spinal cord compression; and (ii) adhesion of the cavity around the expanded blood vessels. Because the veins have a thinner wall and lower blood pressure, they could be occluded easily in comparison to the arteries. Our findings in the present study suggest that circulatory disturbance of the venous system was a more important factor than that of the arterial system. In conclusion, we speculate that the antero-posterior compression produces the condition of spinal canal stenosis which could easily damage the spinal cord.

Our model could be useful in the study on compressive myelopathy.

#### Acknowledgements

The authors thank Masahiko Hashida for his invaluable technical assistance on MR imaging and Yoshinobu Murakami for the preparation of the histological slides. We also gratefully acknowledge the assistance of the staff of The Animal Experimental Institution in Yamaguchi University School of Medicine. No benefits in any form have been received from a commercial party related directly or indirectly to the subject of this study.

## References

- [1] Allen KL. Neuropathies caused by bony spurs in the cervical spine with special reference to surgical treatment. *J Neurol Neurosurg Psychiat* 1952;12:20–36.
- [2] Al-Mefty O, Harkey HL, Marawi I, Haines DE, Peeler DF, Wilner HI, et al. Experimental chronic compressive cervical myelopathy. *J Neurosurg* 1993;79:550–61.
- [3] Arbit E, Galicich W, Galicich JH, Lau N. An animal model epidural compression of the spinal cord. *Neurosurgery* 1989;24:860–3.
- [4] Bailey P, Casarnajor L. Osteoarthritis of the spine as a cause of compression of spinal cord and its roots. *J Nerv Ment Dis* 1911;38:588–609.
- [5] Bedford PD, Bosanquet FD, Ritchie RW. Degeneration of the spinal cord associated with cervical spondylosis. *Lancet* 1952;2:55–9.
- [6] Bennet MH, MacCallum JE. Experimental decompression of spinal cord. *Surg Neurol* 1977;8:63–7.
- [7] Bennet MH. Effects of compression and ischemia on spinal cord evoked potentials. *Exp Neurol* 1983;80:508–19.
- [8] Bradley WG, Banna M. The cervical dural canal. *Br J Radiol* 1968;41:608–15.
- [9] Burrows HR. The sagittal diameter of the spinal canal in cervical spondylosis. *Clin Radiol* 1963;14:77–86.
- [10] Crandall PH, Batzdorf U. Cervical spondylotic myelopathy. *J Neurosurg* 1964;25:57–66.
- [11] Delattre JY, Arbit E, Thaler HT, Rosenblum MK, Posner JB. A dose-response study of dexamethasone in a model of spinal cord compression caused by epidural tumor. *J Neurosurg* 1989;70:920–5.
- [12] Delattre JY, Arbit E, Rosenblum MK, Thaler HT, Lau N, Galicich JH, Posner JB. High dose versus low dose dexamethasone in experimental epidural spinal cord compression. *Neurosurgery* 1988;22:1005–7.
- [13] Ebara S, Yonenobu K, Fujiwara K, Yamashita K, Ono K. Myelopathy hand characterized by muscle wasting: a different type of myelopathy hand in patients with cervical spondylosis. *Spine* 1988;13:785–91.
- [14] Fukuoka M, Matsui N, Otsuka T, Murakami M, Seo Y. Magnetic resonance imaging of experimental subacute spinal cord compression. *Spine* 1998;23:1540–9.
- [15] Gooding MR, Wilson CB, Hoff JT. Experimental cervical myelopathy. Effect of ischemia and compression of the canine cervical cord. *J Neurosurg* 1975;43:9–17.
- [16] Hashizume Y, Kameyama T, Mizuno J, Nakagawa H, Yanagi T, Yoshida M. Pathology of spinal cord lesions caused by ossification of the posterior longitudinal ligament. In: Ono K, editor. *Ossification of the Posterior Longitudinal Ligament*. Tokyo: Springer; 1997. p. 59–64.
- [17] Hinck VC, Sachdev NS. Developmental stenosis of the cervical spinal canal. *Brain* 1966;89:27–36.
- [18] Hukuda S, Wilson CB. Experimental cervical myelopathy. Effects of compression and ischemia on the canine cervical cord. *J Neurosurg* 1972;37:631–52.
- [19] Ito T, Oyanagi K, Takahashi H, Takahashi HE, Ikuta F. Cervical spondylosis myelopathy: clinicopathologic study on the progression pattern and thin myelinated fibers of the lesions of seven patients examined during complete autopsy. *Spine* 1996;21:827–33.
- [20] Jeanmonod D, Sindou M, Mauguier F. The human cervical and lumbo-sacral electrospinogram: data from intraoperative spinal cord surface recordings. *Electroencephalogr Clin Neurophysiol* 1991;80:477–89.
- [21] Kaneko K, Kawai S, Taguchi T, Fuchigami Y, Ito T, Morita H. Correlation between spinal cord compression and abnormal patterns of median nerve somatosensory evoked potentials in compressive cervical myelopathy: comparison of surface and epidurally recorded responses. *J Neurol Sci* 1998;158:193–202.
- [22] Mair WGP, Druckman R. The pathology of spinal cord lesions and their relation to the clinical features in protrusion of cervical intervertebral discs. *Brain* 1953;76:70–91.
- [23] Manabe S, Ohno T, Tanaka H, Park P. Spinal cord compression by epidural metastases. Fibrosacoma experiments in rats. *Acta Orthop Scand* 1988;59:117–21.
- [24] Manabe S, Tanaka H, Higo Y, Park P, Ohno T, Tateishi A. Experimental analysis of the spinal cord compressed by spinal metastasis. *Spine* 1989;14:1308–15.
- [25] Munro D. Relation between spondylosis cervicalis and its contents. *New Eng J Med* 1960;262:839–46.
- [26] Nugent GR. Clinicopathologic correlation in cervical spondylosis. *Neurology* 1959;9:273–81.
- [27] Nurick S. The natural history of the neurological complications of cervical spondylosis. *Brain* 1972;95:87–100.
- [28] Ogino H, Tada K, Okada K, Yonenobu K, Yamamoto T, Ono K, Namik H. Canal diameter, antero-posterior compression ratio, and spondylotic myelopathy of the cervical spine. *Spine* 1983;8:1–15.
- [29] Payne LW, Spillane JD. The cervical spine, an anatomical study of 70 specimens, with particular reference to the problem of cervical spondylosis. *Brain* 1957;80:571–96.
- [30] Penning L. Some aspects of the cervical spine in chronic myelopathy. *Neurology* 1962;12:513–9.
- [31] Satomi K, Okuma T, Kenmotsu K, Nakamura Y, Hirabayashi K. Level diagnosis of cervical myelopathy using evoked spinal cord potentials. *Spine* 1988;13:1217–24.
- [32] Schramm J, Shigeno T, Brock M. Clinical signs and evoked response alterations associated with chronic experimental cord compression. *J Neurosurg* 1983;58:734–41.
- [33] Shimoji K, Higashi H, Kato T. Epidural recording of spinal electrogram in man. *Electroencephalogr Clin Neurophysiol* 1971;30:236–9.
- [34] Shinomiya K, Furuya K, Sato R, Okamoto A, Kurosa Y, Fuchioka M. Electrophysiologic diagnosis of cervical OPLL myelopathy using evoked spinal cord potentials. *Spine* 1988;11:1225–33.
- [35] Shinomiya K, Mutoh N, Furuya K. Study of experimental cervical spondylotic myelopathy. *Spine* 1992;17(10S):S383–7.
- [36] Stoops WL, King RB. Neural complications of cervical spondylosis. Their response to laminectomy and foraminotomy. *J Am Med Assoc* 1955;192:281–4.
- [37] Symonds CP. Interrelation of trauma and cervical spondylosis in compression of cervical cord. *Lancet* 1953;1:451–5.
- [38] Tarlov LM, Klinger H, Vitale S. Spinal cord compression studies. *Arch Neurol Psychiat* 1953;70:813–9.
- [39] Taylor AR. Mechanism and treatment of spinal cord disorders associated with cervical spondylosis. *Lancet* 1953;1:717–20.
- [40] Ushio Y, Posner R, Posner JB, Shapiro WR. Experimental spinal cord compression by epidural neoplasms. *Neurology* 1977;27:422–9.
- [41] Wilkinson M. The morbid anatomy of cervical spondylosis and myelopathy. *Brain* 1960;83:589–616.
- [42] Wolf BS, Khilnani M, Malis L. The sagittal diameter of the bony cervical spinal canal and its significance in cervical spondylosis. *J Mount Sainai Hospital* 1956;23:283–92.
- [43] Yu YL, Boulay JM, Stevens JM, Kendall BE. Computer-assisted myelography in cervical spondylotic myelopathy and radiculopathy. *Brain* 1986;109:259–78.